

POSSIBLE ORIGIN OF THE G2 CLOUD FROM THE TIDAL DISRUPTION OF A KNOWN GIANT STAR BY SGR A*

JAMES GUILLOCHON^{1,2}, ABRAHAM LOEB¹, MORGAN MACLEOD³, ENRICO RAMIREZ-RUIZ³*Draft version September 17, 2018*

ABSTRACT

The discovery of the gas cloud G2 on a near-radial orbit about Sgr A* has prompted much speculation on its origin. In this *Letter*, we propose that G2 formed out the debris stream produced by the removal of mass from the outer envelope of a nearby giant star. We perform hydrodynamical simulations of the returning tidal debris stream with cooling, and find that the stream condenses into clumps that fall to Sgr A* approximately once per decade. We propose that one of these clumps is the observed G2 cloud, with the rest of the stream being detectable at lower Br γ emissivity along a trajectory that would trace from G2 to the star that was partially disrupted. By simultaneously fitting the orbits of S2, G2, and $\sim 2,000$ candidate stars, and by fixing the orbital plane of each candidate star to G2 (as is expected for a tidal disruption), we find that the late-type star S1-34 has an orbit that is compatible with the notion that it was tidally disrupted to produce G2. If S1-34 is indeed the star that was disrupted, it last encountered Sgr A* in the late 18th century, and will likely be disrupted again in several hundred years. However, while S1-34's orbit is compatible with the giant disruption scenario given its measured position and proper motion, its radial velocity is currently unknown. If S1-34's radial velocity is measured to be compatible with a disruptive orbit, it would strongly suggest that a tidal disruption of S1-34 produced G2.

Subject headings: black hole physics — galaxies: active — gravitation

1. INTRODUCTION

Only 1% of supermassive black holes accrete at rates comparable to their Eddington limits (Ho 2008). Sgr A*, a $\sim 4 \times 10^6 M_\odot$ black hole lying at the center of our galaxy (Ghez et al. 1998; Genzel et al. 2000), is no exception, and is thought to be accreting only 10^{-9} to $10^{-6} M_\odot \text{ yr}^{-1}$ (Narayan et al. 1998; Yuan & Narayan 2014). Given this small accretion rate, it was surprising to discover an Earth-mass cloud (G2) in a disruptive orbit about Sgr A* (Gillessen et al. 2012), as its destruction would deposit a mass around Sgr A* at a rate comparable to its steady accretion rate.

Because G2's low density places it well within its tidal disruption radius at the time of its discovery, it has been proposed that it requires a star at its center to maintain its compactness (Murray-Clay & Loeb 2011). However, the non-detection of a host star with $K \lesssim 20$ limits the kinds of stars that can reside within it (Meyer et al. 2013, although see Eckart et al. 2013), and is comparable to the brightness expected for a young T-Tauri star, which could host a protoplanetary disk (Murray-Clay & Loeb 2011) or produce a wind (Ballone et al. 2013; Scoville & Burkert 2013).

When a star is disrupted by a supermassive black hole, material that is removed from it collimates into a thin stream that feeds the black hole for centuries at a rate greater than Sgr A*'s steady accretion rate (Guillochon & Ramirez-Ruiz 2013; Guillochon et al. 2013). We propose that G2 is associated with a star that is not contained within it, but is rather a starless clump within a long stream resulting from the disruption of a star over two centuries ago. Because G2's periape distance $r_p \sim 100$ AU, this would necessarily be a large giant with $R_* \sim 1$ AU. In this scenario, G2 is one of dozens of

clouds that have fallen onto Sgr A* on similar orbits, with the accretion rate likely being larger in the past, closer to the time of disruption. Indeed, X-ray light echoes suggest that Sgr A* was far more active centuries ago (Ryu et al. 2013). We show that the giant star S1-34 (Rafelski et al. 2007; Schödel et al. 2009; Yelda et al. 2010; Do et al. 2013), which in projection lies along the path of a stream of clumps discovered in K that are spatially coincident with a Br γ detection (Gillessen et al. 2013a; Meyer et al. 2013), is both large enough to lose mass at G2's periape, and possesses a proper motion and position that are compatible with a tidally disruptive orbit.

The work presented in this *Letter* is composed of two parts: A demonstrative hydrodynamical simulation of the return of a debris stream resulting from a tidal disruption of a giant star, and a systematic search to find a star whose orbit is compatible with the giant disruption scenario. In Section 2 we show that the debris stream resulting from a giant disruption can produce both a G2-like clump on a Keplerian trajectory, and an extended tail structure whose shape is determined by the range of binding energies within the tidal tail. In Section 3 we present a systematic search of large giants within our galactic center (GC), and explain why S1-34's properties are highly suggestive that it was tidally disrupted. In Section 4 we discuss implications of G2 being produced by the disruption of a giant.

2. SIMULATION OF A TIDAL STREAM IN THE GC

2.1. Setup

We perform a hydrodynamical simulation of a debris stream returning to Sgr A* in FLASH⁴, a well-tested adaptive mesh code for astrophysical fluid problems (Fryxell et al. 2000). We presume a black hole of mass $M_h = 4.3 \times 10^6 M_\odot$ and set our background temperature profile based on measurements of diffuse X-ray emission in the GC (Equation 2 of Anninos et al. 2012). The GC is thought to be convec-

jguillochon@cfa.harvard.edu

¹ Harvard-Smithsonian Center for Astrophysics, The Institute for Theory and Computation, 60 Garden Street, Cambridge, MA 02138, USA² Einstein Fellow³ Department of Astronomy and Astrophysics, University of California, Santa Cruz, CA 95064⁴ Movies available at <http://goo.gl/58iEFX>.

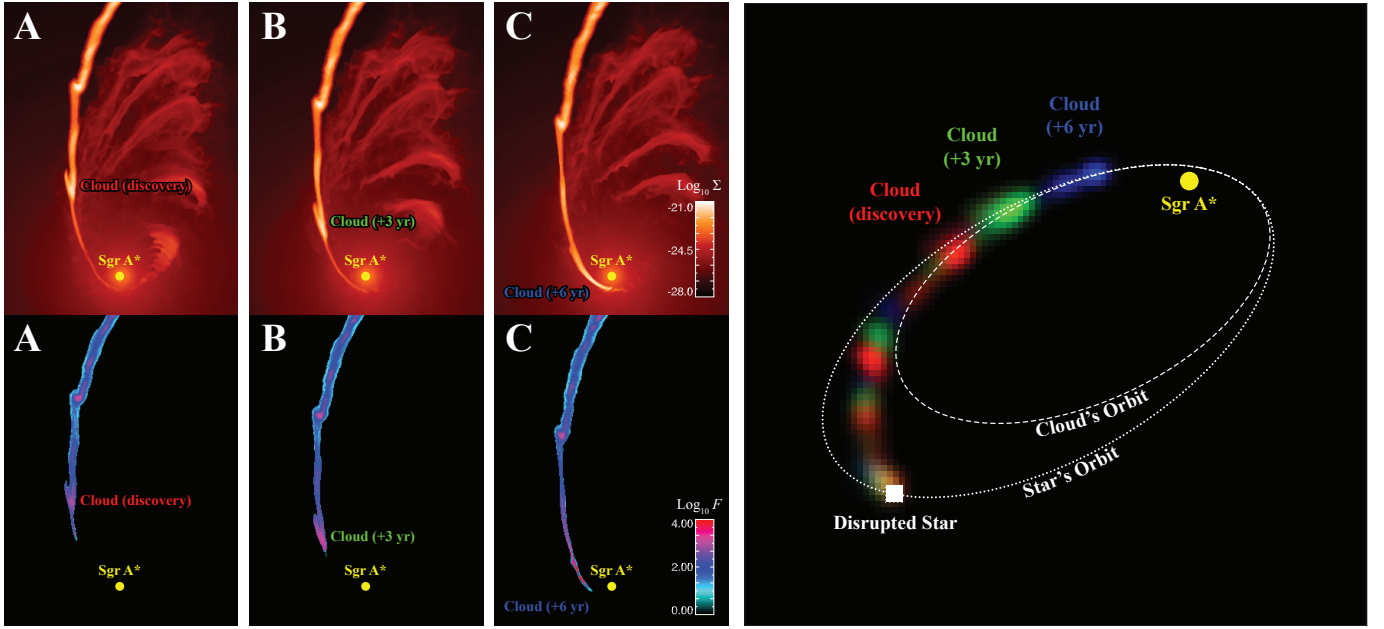


FIG. 1.— Snapshots from a hydrodynamical simulation demonstrating the dynamics of a returning stream produced by the disruption of a giant star. In the left six panels (labeled A, B, and C) we show a time-sequence of the returning gas, with the surface density Σ shown in the top panels and total line-cooling flux F shown in the bottom panels. Labeled in each panel is a prominent cloud that forms within the stream, falling onto the black hole over a period of ~ 6 yr. In the right panel we show $F_{\text{Br}\gamma}$, with the simulation volume rotated such that its projection matches the best-fitting orientation for the G2 cloud as found by our MLA, smoothed over 100 AU (33 AU per pixel). In addition to the lead cloud, there are a trail of clouds that follow it, but not on a path identical to leading cloud.

tively unstable, which has been treated in previous simulations of G2 by either artificially resetting the background to a constant profile at every timestep (Burkert et al. 2012; Schartmann et al. 2012; Ballone et al. 2013), or by simulating for a short period of time such that convective instability does not develop (Abarca et al. 2013). Because we were concerned that the growth of instability within the stream might be affected by an ad-hoc relaxation scheme, our approach is different from the aforementioned works. As in Anninos et al. (2012), we set $\rho = 1.3 \times 10^{-21} \eta$ (where we set $\eta = 1$) at $r = 1.3 \times 10^{16}$ cm, but we presume a slightly steeper profile than the profile motivated by observations, $\rho \propto r^{-3/2}$. However, this configuration is stable to convection, obviating the need to artificially stabilize the background medium, and permitting unfettered evaluation of the growth of hydrodynamical stream instabilities. Our choice affects the distance from Sgr A* at which instability will grow as growth is dependent on the ratio of densities between the two fluids, but should not affect the growth qualitatively.

When a star is partially disrupted, the mass it loses is distributed within a thin stream with a range of binding energies (MacLeod et al. 2013). This stream remains thin as it leaves the vicinity of the black hole, so long as its evolution is adiabatic (Kochanek 1994; Guillochon et al. 2013). Unlike main sequence (MS) disruptions, giant disruptions produce streams that are initially much less dense, resulting in a stream that quickly becomes optically thin. Once optically thin, the stream’s internal energy is set by the ionizing radiation from stars and gas in the surrounding GC environment, which floors the temperature of the gas component to $\sim 10^4$ K. At the same time, the stream cools via recombination lines, with the cooling rate Λ having a dependence on metallicity, temperature, and optical depth (Sutherland & Dopita 1993; Shcherbakov 2013). We approximate Λ as a Gaussian func-

tion of the temperature T centered about 10^5 K,

$$\Lambda = 10^{-21} \frac{\rho}{\mu_e^2 m_p^2} \exp \left[-\frac{9}{2} (\log T - 5)^2 \right] \text{ erg cm}^3 \text{ s}^{-1}, \quad (1)$$

where ρ is the density and μ_e is the molecular weight per electron. In regions of sufficient density photoionization is balanced by recombination, and the stream equilibrates to a temperature of $\sim 10^4$ K.

As the envelopes of giants that are removed upon disruption have negligible self-gravity (MacLeod et al. 2012), the self-gravity of the stream is irrelevant, and thus the stream evolves isothermally Sgr A*’s tidal gravity. The density profile of such a stream is

$$\rho(s, r) = \rho_0(r) \exp \left[-\frac{\mu_h s^2 m_p \mu_e}{2 r^3 k_b T} \right], \quad (2)$$

where s is the cylindrical distance from the center of the stream, r is the distance to the black hole, $\mu_h \equiv GM_h$ is the standard gravitational parameter, and μ is the mean molecular weight.

Our simulations feed matter to the black hole via a moving boundary condition with a cylindrical profile as determined by Equation 2, where the boundary lies at the apoapse of each fluid element, and is oriented perpendicular to the gas motion, set initially to the $-x$ direction. The boundary moves outwards such that its distance $r = (t/t_i)^{2/3}$, where $t_i \equiv 2\pi \sqrt{a^3/GM_h}$. We set the mass feeding rate to be equal to $3M_\oplus$ per decade, the rate implied by the accretion of one G2-sized cloud.

2.2. Results

At some distance from Sgr A*, the ambient gas pressure becomes competitive with the internal pressure of the stream, establishing pressure equilibrium between the stream and its surroundings. This enables the development of Kelvin-Helmholtz instabilities within the stream (Chandrasekhar

1961), producing over (under) densities developing at the crests (troughs) of the instabilities (Figure 1). Because the cooling rate is enhanced with greater density (Equation 1), the density perturbations in the stream are amplified, eventually resulting in a fragmented stream with dense clumps separated by tenths of arcseconds. These clouds fall towards Sgr A* in balance with the ambient pressure, and eventually succumb to tidal forces, stretching significantly (Figure 1, top three panels). Throughout this evolution, the total flux emitted by the clouds is approximately constant (Figure 1, bottom three panels), resulting in a cloud whose properties seem to vary little over a period of years (Figure 1, right panel), as is observed for G2 (Gillessen et al. 2012).

As matter is continually fed to the black hole after a disruption, new clumps form continually form out of the stream. If G2 formed in this manner, it is one of many clumps that accreted onto Sgr A* over the preceding centuries, and is unique only in the sense that it is the particular clump we happen to observe returning to Sgr A* at the present epoch. Rather than each clump generating a strong bow shock in the ambient medium, the clumps along a fixed path cleared of ambient gas by previously accreted clumps, which would explain its non-detection in the radio (Sadowski et al. 2013; Akiyama et al. 2013). Each clump is tidally stretched and heated as it passes periape, resulting in an increase in temperature above 10^5 K, rendering them invisible in recombination lines, but potentially detectable in X-rays (Anninos et al. 2012).

3. ORBIT FITTING

If the formation of G2 is due to the partial disruption of a star, its initial orbital orientation, defined by the inclination i , argument of periape ω , longitude of the ascending node Ω , and its initial pericenter distance r_p will be identical to the original star's. However, because the G2 clump originates from some piece of the debris stream that is more bound to Sgr A* than the star that produced it, its specific orbital energy ϵ will be larger by a factor $\Delta\epsilon$, which means that the semimajor axis a of G2 is restricted to values smaller than the star it originated from. Hence, if G2's orbital elements and the position/velocity of Sgr A* were known, there is a single free parameter a .

As G2's orbital parameters and the position of Sgr A* are only known to some precision, finding a star whose orbit is compatible with G2's orbit requires simultaneously determination of G2's orbital elements (six parameters), Sgr A*'s position, velocity, and mass (seven parameters), and the candidate star's a . Because the error bars on G2's position are too great to constrain Sgr A* alone, we also simultaneously fit the orbital parameters of the short-period star S2 (six parameters), as is done in Phifer et al. (2013) and Gillessen et al. (2013b). This enables a precise determination of Sgr A*'s position, and allows one to calibrate the reference frame (Gillessen et al. 2009a). However, the errors in M_h and distance to the GC R_0 are rather large when using S2 alone, so we additionally use priors of $M_h = 4.31 \pm 0.42 \times 10^6 M_\odot$ and $R_0 = 8.33 \pm 0.35$ kpc as determined by Gillessen et al. (2009b). As in that paper, we assume a prior on Sgr A*'s radial velocity $v_r = 0 \pm 5$ km/s.

Lastly, our fitting includes two additional free parameters to measure any extra variance in G2's position and radial velocity. This is motivated by the change in time in the reported orbital elements of G2, suggesting that the measurement error bars may not capture the full uncertainty in G2's position. This may either arise from deviations from a pure Keplerian orbit, as might be expected when the cloud interacts with the

gas surrounding Sgr A* (Abarca et al. 2013), or if the Br γ emission does not follow the mass (Phifer et al. 2013). In total, our model includes 22 free parameters.

We then run independent maximum-likelihood analyses (MLAs) using *emcee* (Foreman-Mackey et al. 2013) with each MLA presuming that a star of the catalogue of Schödel et al. (2009) may be the star that was tidally disrupted to produce the G2 cloud. Schödel et al. (2009) provides a single position and proper motion estimate for each star for the reference year 2004.44 and is $\sim 80\%$ complete for stars with $K \sim 13$ (Do et al. 2009). We exclude stars with either $K > 16$ (as these stars are too small to lose mass at G2's periape), stars whose proper motions are greater than the escape velocity from Sgr A* at their observed position, and stars with positive declination. In total we consider 1,727 stars. For this *Letter* our MLAs utilize the positions and velocities of G2 and S2 reported in Gillessen et al. (2009a, 2013a,b)⁵, Ghez et al. (2008), and Phifer et al. (2013); the combination of these datasets required repeating the alignment procedure of Gillessen et al. (2009a) to account for relative proper motion between the two observing frames. We then sort the stars based on their MLA scores.

3.1. A Candidate Late-Type Star: S1-34

Most of the stars of Schödel et al. (2009) can be immediately rejected as either their positions or proper motions are not consistent with a star who shares five of six of G2's orbital elements. Some fraction of the stars have orbits that are almost compatible with G2's, but only when allowing r_p of the candidate to differ from G2's (i.e. by adding another free parameter). The addition of r_p as a free parameter may be physically motivated as G2 could deviate from its original Keplerian trajectory, but observations show that its path is largely consistent with Keplerian and that G2's original periape does not differ from its measured periape by more than a factor of ~ 2 (Meyer et al. 2013; Phifer et al. 2013; Gillessen et al. 2013b).

When forcing r_p of a candidate to be equal to G2's periape, we find that only a single late-type star is compatible with G2: S1-34 (Figure 2). Originally classified as an early-type star (Rafelski et al. 2007), it was recently re-classified as a late-type star upon discovery of a weak Na I doublet (Do et al. 2013), suggesting that it is a "warm" giant with a surface temperature of $\sim 5,000$ K. We estimate the star's bolometric correction to be 1.9 in K (Buzzoni et al. 2010), and combined with the average K extinction in the GC of ~ 2.5 magnitudes (Schödel et al. 2010), its apparent K magnitude of 13.1 suggests an absolute magnitude of -5.9 (assuming 8.3 kpc to the GC) and thus a physical radius of ~ 1 AU.

As an additional verification that S1-34 is compatible with a tidally-disruptive orbit, we separately performed an MLA with the position and proper motions reported in Yelda et al. (2010) (Figure 2, bottom three panels). The position reported by Yelda et al. for S1-34 does not agree within the error bars with that of Schödel et al. (2009), and while the most-likely solution of Yelda et al. suggests S1-34 is bound to Sgr A*, approximately 35% of our solutions suggest that S1-34 may be unbound. Therefore, we can only report a lower-limit for a , eccentricity e , and period P of S1-34 when using Yelda et al.. Given the disagreement between the two datasets, it is clear that S1-34's period can only be determined by better characterizing the systematic errors in S1-34's position.

⁵ Publicly available at <https://wiki.mpe.mpg.de/gascloud>

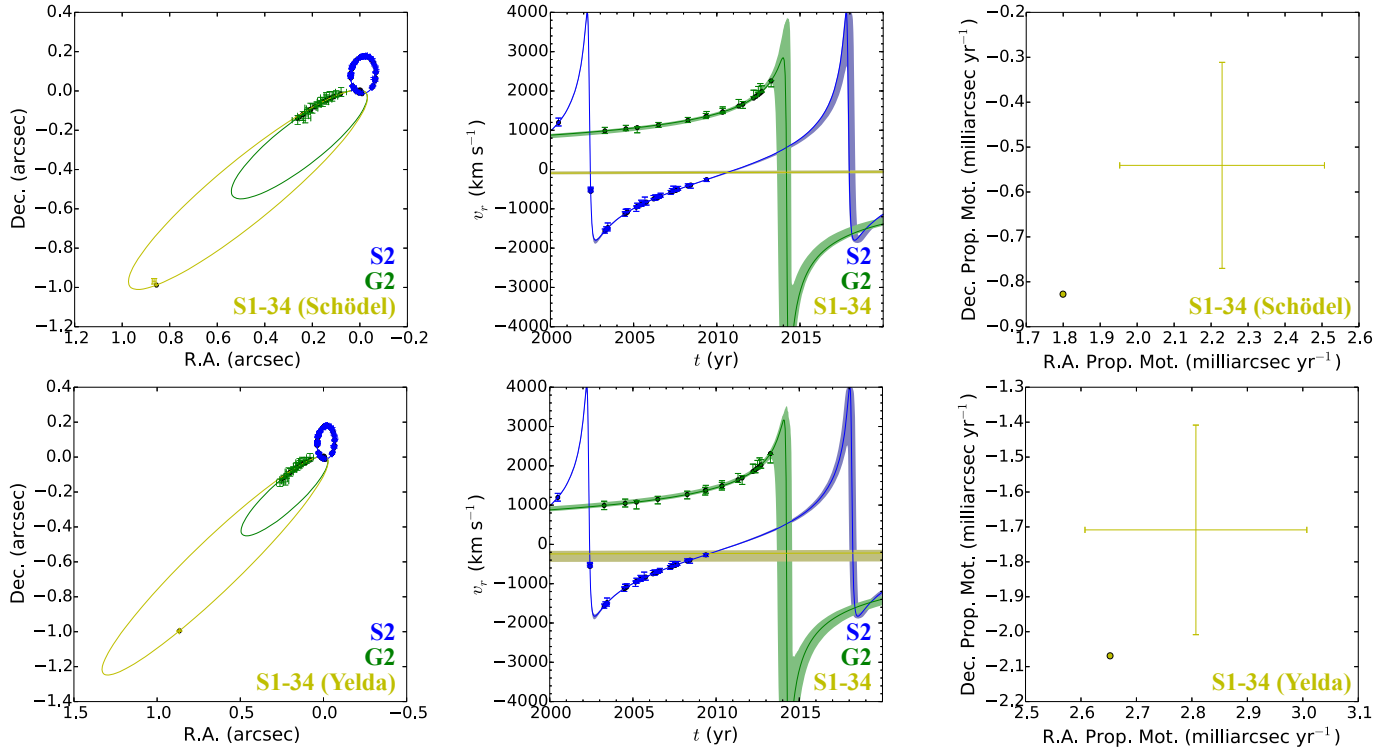


FIG. 2.— Results from simultaneous fits of S2, G2, and S1-34, with the three objects being colored blue, green, and yellow respectively (Sgr A*’s position is shown with a black point). The points with error bars are the observational data, whereas the filled circles are the positions of the objects according to our model. The top three panels show the fitting results when the position/proper motion of S1-34 reported in Schödel et al. (2009) is used, whereas the bottom three panels show the results when Yelda et al. (2010) is used. The left panels show the sky-projected paths of the three objects for the maximum likelihood fit, with x and y corresponding to right ascension and declination. The middle panels show the velocity along the line of sight v_r , with the shaded regions indicating the $2\text{-}\sigma$ error bars in v_r as a function of time. The right panels show the proper motion measurement of S1-34, with the error bars corresponding to observations and the filled circle to the model.

TABLE 1
TABLE OF ESTIMATED ORBITAL PROPERTIES FOR G2 AND S1-34

Name	P (yr)	r_p (r_g)	$t_{p,0}$ (yr) ^a	$t_{p,1}$ (yr) ^b	a (mpc)	e	i ($^\circ$)	Ω ($^\circ$)	ω ($^\circ$)
G2 ^c	232 ± 30	900 ± 270	1782 ± 30	2014.21 ± 0.21	30.9 ± 2.5	0.9863 ± 0.0034	117.0 ± 4.4	101.8 ± 11.0	105.6 ± 4.7
S1-34 ^c	561 ± 131	“ ”	“ ”	2341 ± 108	55.8 ± 6.8	0.9924 ± 0.0020	“ ”	“ ”	“ ”
G2 ^d	242 ± 41	1130 ± 330	1772 ± 41	2014.23 ± 0.24	31.4 ± 3.3	0.9843 ± 0.0037	106.7 ± 6.2	85.2 ± 9.2	109.0 ± 2.1
S1-34 ^d	$> 630.0^e$	“ ”	“ ”	$> 2447^e$	$> 60.0^e$	$> 0.9899^e$	“ ”	“ ”	“ ”

^aPrevious encounter date.

^bNext encounter date.

^cS1-34 from Schödel et al. (2009).

^dS1-34 from Yelda et al. (2010).

^e $2\text{-}\sigma$ lower limit.

Radial velocities are known for a small subset of stars in the GC (Gillessen et al. 2009a; Lu et al. 2009; Do et al. 2013). At the present, radial velocity data is not publicly available for S1-34, but our model affirms that its velocity would presently be between -400 (using Yelda et al.) and -30 (using Schödel et al.) km s^{-1} . If its radial velocity is measured to be external to these values, its association with G2 could be ruled out. If S1-34 is not the star that produced G2, there are only a few other stars in the nuclear cluster whose orbits are potentially compatible and are large enough to lose mass at G2’s periaapse, but our MLA suggests that these stars either have apocenters that lie exterior to Sgr A*’s sphere of influence, or require that $r_{p,\text{candidate}} \neq r_{p,\text{G2}}$. As is the case for a fraction of our Yelda et al. solutions, systematic errors may prevent the determination of bound solutions for other candidates.

In Figure 3 we show evolution tracks of various stellar

masses generated using MESA (Paxton et al. 2011, 2013) as compared to the distribution of G2 periaapse distances produced by fitting procedure. The dashed gray line shows the approximate luminosity of S1-34, which suggests a giant with a stellar mass between $10 - 16 M_\odot$. Assuming $M_* = 10 M_\odot$, $R_* = 1 \text{ AU}$, and that the giant would begin to lose mass when $r_p/r_t = 2$ (MacLeod et al. 2012), yields a periaapse distance of $2 \times 10^3 r_g$, slightly larger than the r_p from our MLA (Table 1).

Recently, it has been noted that the tail-like feature that lies in G2’s wake extends far beyond G2’s orbital ellipse, which Meyer et al. (2013) argued is evidence that it is unassociated with G2. However, the giant disruption scenario predicts that an extended tail should connect G2 to the star that was disrupted, and this tail should *not* be cospatial with G2’s trajectory (Figure 1), nor possess the same radial velocity. In projection, S1-34 seemingly lies within $0.1''$ of the observed tail. While not proof that the feature is genuinely associated with

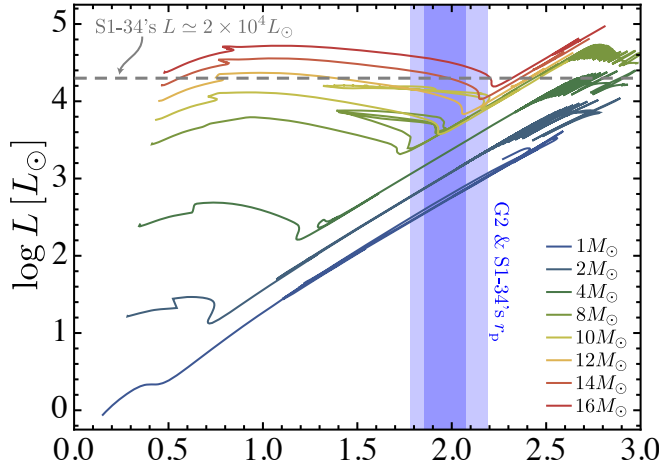


FIG. 3.— Luminosity L vs. pericenter distance r_p (where we have assumed $r_p/r_t = 2$) diagram of stars of various masses as compared to the fitted pericenter distances of G2/S1-34. The blue regions correspond to the 1- and 2- σ scatter about the median fit of Schödel et al. (2009). The approximate bolometric luminosity of S1-34 is shown by the dashed grey line.

either G2 or S1-34, it is highly suggestive.

4. IMPLICATIONS

The minimum amount of mass the star needs to lose to produce the G2 cloud is approximately equal to the average accretion rate from the disruption of one G2 cloud extended to

the time of disruption ~ 200 yr ago, this suggests that S1-34 needed to lose at least $\sim 30M_\oplus$ at the time of disruption. This mass is small compared to the amount available in a $\sim 10M_\odot$ giant, suggesting that S1-34 could have “spoon-fed” Sgr A* for tens of millions of years (MacLeod et al. 2013). This repeated interaction greatly increases the rate G2-like clumps would be detectable, as there are always likely to be a few giant stars on such orbits at any time, and always some clouds forming within their host debris streams.

If the giant disruption scenario for G2 is correct, it suggests that a very large fraction of the material deposited within 100 AU of Sgr A* over the past two centuries may have come from a single star. If this material is capable of circularizing and subsequently accreting onto the black hole, giant disruptions may explain a large fraction of low-level supermassive black hole activity in the local universe.

We thank L. Meyer and S. Gillessen for assistance in interpreting the observational data. This work was supported by Einstein grant PF3-140108 (J.G.), NSF grant AST-1312034 (A.L.), and NSF GFRP (M.M.).

REFERENCES

- Abarca, D., Sadowski, A., & Sironi, L. 2013, arXiv, 2313
Akiyama, K., Kino, M., Sohn, B. W., et al. 2013, arXiv, 5852
Anninos, P., Fragile, P. C., Wilson, J., & Murray, S. D. 2012, ApJ, 759, 132
Ballone, A., Schartmann, M., Burkert, A., et al. 2013, arXiv, 1305.7238v1
Burkert, A., Schartmann, M., Alig, C., et al. 2012, ApJ, 750, 58
Buzzoni, A., Patelli, L., Bellazzini, M., Pecci, F. F., & Oliva, E. 2010, MNRAS, 403, 1592
Chandrasekhar, S. 1961, International Series of Monographs on Physics
Do, T., Ghez, A. M., Morris, M. R., et al. 2009, ApJ, 703, 1323
Do, T., Lu, J. R., Ghez, A. M., et al. 2013, ApJ, 764, 154
Eckart, A., Horrobin, M., Britzen, S., et al. 2013, arXiv, 2753
Foreman-Mackey, D., Hogg, D. W., Lang, D., & Goodman, J. 2013, PASP, 125, 306
Fryxell, B., Olson, K., Ricker, P., et al. 2000, ApJS, 131, 273
Genzel, R., Pichon, C., Eckart, A., Gerhard, O. E., & Ott, T. 2000, MNRAS, 317, 348
Ghez, A. M., Klein, B. L., Morris, M., & Becklin, E. E. 1998, ApJ, 509, 678
Ghez, A. M., Salim, S., Weinberg, N. N., et al. 2008, ApJ, 689, 1044
Gillessen, S., Eisenhauer, F., Fritz, T. K., et al. 2009a, ApJ, 707, L114
Gillessen, S., Eisenhauer, F., Trippe, S., et al. 2009b, ApJ, 692, 1075
Gillessen, S., Genzel, R., Fritz, T. K., et al. 2012, Nature, 481, 51
—. 2013a, ApJ, 763, 78
—. 2013b, ApJ, 774, 44
Guillochon, J., Manukian, H., & Ramirez-Ruiz, E. 2013, arxiv
Guillochon, J., & Ramirez-Ruiz, E. 2013, ApJ, 767, 25
Ho, L. C. 2008, ARA&A, 46, 475
Kochanek, C. S. 1994, ApJ, 422, 508
Lu, J. R., Ghez, A. M., Hornstein, S. D., et al. 2009, ApJ, 690, 1463
MacLeod, M., Guillochon, J., & Ramirez-Ruiz, E. 2012, ApJ, 757, 134
MacLeod, M., Ramirez-Ruiz, E., Grady, S., & Guillochon, J. 2013, ApJ, 777, 133
Meyer, L., Ghez, A. M., Witzel, G., et al. 2013, arXiv, 1715
Murray-Clay, R. A., & Loeb, A. 2011, arXiv, 4822
Narayan, R., Mahadevan, R., Grindlay, J. E., Popham, R. G., & Gammie, C. 1998, ApJ, 492, 554
Paxton, B., Bildsten, L., Dotter, A., et al. 2011, ApJS, 192, 3
Paxton, B., Cantiello, M., Arras, P., et al. 2013, ApJS, 208, 4
Phifer, K., Do, T., Meyer, L., et al. 2013, ApJ, 773, L13
Rafelski, M., Ghez, A. M., Hornstein, S. D., Lu, J. R., & Morris, M. 2007, ApJ, 659, 1241
Ryu, S. G., Nobukawa, M., Nakashima, S., et al. 2013, PASJ, 65, 33
Sadowski, A., Sironi, L., Abarca, D., et al. 2013, MNRAS, 432, 478
Schartmann, M., Burkert, A., Alig, C., et al. 2012, ApJ, 755, 155
Schödel, R., Merritt, D., & Eckart, A. 2009, A&A, 502, 91
Schödel, R., Najarro, F., Muzic, K., & Eckart, A. 2010, A&A, 511, A18
Scoville, N., & Burkert, A. 2013, ApJ, 768, 108
Shcherbakov, R. V. 2013, arXiv, 2282
Sutherland, R. S., & Dopita, M. A. 1993, ApJS, 88, 253
Yelda, S., Lu, J. R., Ghez, A. M., et al. 2010, ApJ, 725, 331
Yuan, F., & Narayan, R. 2014, arxiv